Two-Dimensional Model Test Study of New Western Breakwater Proposal for Port of Hanstholm

Eldrup, Mads Røge; Andersen, Thomas Lykke

Publication date:
2016

Document Version
Publisher's PDF, also known as Version of record

DEPARTMENT OF CIVIL ENGINEERING
AALBORG UNIVERSITY

Two-Dimensional Model Test Study of New Western Breakwater Proposal for Port of Hanstholm

M. R. Eldrup
T. Lykke Andersen

Carried out under contract for:

Rambøll Denmark A/S

DCE Contract Report No. 184

Aalborg University
Department of Civil Engineering
Division of Division of Reliability, Dynamics and Marine Engineering

DCE Contract Report No. 184

Two-Dimensional Model Test Study of New Western Breakwater Proposal for Port of Hanstholm

by

M. R. Eldrup
T. Lykke Andersen

December 2016

Scientific Publications at the Department of Civil Engineering

Technical Reports are published for timely dissemination of research results and scientific work carried out at the Department of Civil Engineering (DCE) at Aalborg University. This medium allows publication of more detailed explanations and results than typically allowed in scientific journals.

Technical Memoranda are produced to enable the preliminary dissemination of scientific work by the personnel of the DCE where such release is deemed to be appropriate. Documents of this kind may be incomplete or temporary versions of papers—or part of continuing work. This should be kept in mind when references are given to publications of this kind.

Contract Reports are produced to report scientific work carried out under contract. Publications of this kind contain confidential matter and are reserved for the sponsors and the DCE. Therefore, Contract Reports are generally not available for public circulation.

Lecture Notes contain material produced by the lecturers at the DCE for educational purposes. This may be scientific notes, lecture books, example problems or manuals for laboratory work, or computer programs developed at the DCE.

Theses are monograms or collections of papers published to report the scientific work carried out at the DCE to obtain a degree as either PhD or Doctor of Technology. The thesis is publicly available after the defence of the degree.

Latest News is published to enable rapid communication of information about scientific work carried out at the DCE. This includes the status of research projects, developments in the laboratories, information about collaborative work and recent research results.

Published 2016 by
Aalborg University
Department of Civil Engineering
Thomas Manns Vej 23
DK-9220 Aalborg Ø, Denmark

Printed in Aalborg at Aalborg University

DCE Contract Report No. 184

CONTENTS

1 INTRODUCTION

The present report presents results from a two-dimensional model test study carried out at Aalborg University in December 2016 with the proposed trunk section for the new western breakwater in Port of Hanstholm. The objectives of the model tests were to study the stability of the armour layer, toe erosion, overtopping and transmission. The scale used for the model tests was 1:61.5. Unless otherwise specified all values given in this report are prototype values converted from the model to prototype according to the Froude model law.

The model tests were carried out by Ph.D. student Mads Røge Eldrup and Associate Professor, Ph.D. Thomas Lykke Andersen. Technicians Nikolaj Holk, Leif Mortensen and Kim Pour assisted in the laboratory.

On December 8th, Peter Bak Frederiksen and Jørgen Quvang Harck Nørgaard from Rambøll and Niels Clemensen, Peter Nymann and some local fishermen's from Hanstholm Harbour visited the laboratory for observing some of the tests.

In addition to the written report the digital appendices are providing pictures with damage detection and wave analysis documentation for each test.

For further information contact Thomas Lykke Andersen (tla@civil.aau.dk).

2 DESIGN SEA STATES

The client provided 11 design sea states to be tested cf. Table 1.

Table 1: Design sea states (target values).

Target sea state	Water level (m)	Significant wave Height, H_{m0} (m)	Peak wave period, T_P (s)	Corresponding return period
S1	-0.5	5.2	15	1
S2	1.3	5.2	15	1
S3	1.7	5.2	15	1
S4	-0.5	6.5	16	10
S5	1.3	6.5	16	10
S6	1.7	6.5	16	10
S7	-0.5	8.2	16.5	100
S8	1.3	8.2	16.5	100
S9	1.7	8.2	16.5	100
S10	-1	8.2	18	Overload
S11	2.5	8.2	18	Overload

3 SETUP OF THE MODEL TEST

A two-dimensional model was constructed in scale 1:61.5 in a 1.2 m wide and 18.64 m long wave flume at Aalborg University. Fig. 1 shows the test setup in the flume with the breakwater, bathymetry, resistance type wave gauges and overtopping tank. The 1:30 slope used in the model setup reflects the steepest profile measured at the site (value given by client). This steep slope also makes it possible to generate the depth limited conditions in the model tests. The bed near the wavemaker was horizontal corresponding to 37.7 m water depth (CD) in prototype. From this depth, the depth decreased to the toe of the breakwater by a 1:30 foreshore followed by a horizontal seabed. The bathymetry partly consists of a fixed floor and partly of an erodible bed (see Fig. 1). The depth was 11 m (CD) at the toe of the breakwater initially, but increased during testing due to scouring at the toe. The placement of the wave gauges is restricted as a minimum distance of 3h in front of the wavemaker for insignificant nearfield disturbance is needed. Moreover, a minimum distance of $0.4L_P$ from the breakwater as suggested by Klopman and Van der Meer (1999) is used for the model tests. After the first 11 tests a wave gauge was placed at the toe to measure the total $H_{2\%}/H_{1/3}$.

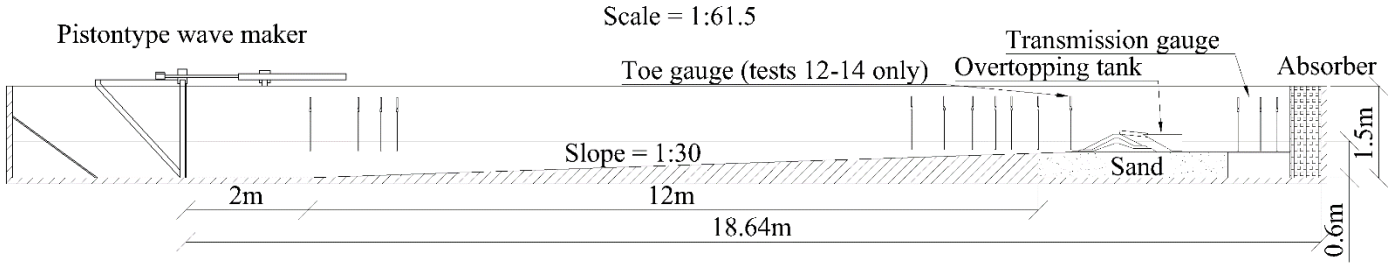

Figure 1: Flume layout. Measures in model scale.

3.1 SCALING

The length scale of the model is a compromise of scale effects and model size (model effects). If the model size is too small viscous scale effects will occur. Therefore, Reynolds number should not be smaller than a critical value which for armour stability is typically taken as $3 \cdot 10^4$.

$$Re = \frac{(gH_{m0})^{0.5} D_n}{\nu} > 3 \cdot 10^4 \quad (1)$$

Where:

Re is the Reynolds number,
g is the gravity acceleration, app. 9.8 m/s^2,
H_{m0} is the significant wave height,
D_n is the nominal diameter of the armour units, i.e. the equivalent cube side length,
ν is the kinematic viscosity, app. 10^{-6} m^2/s.

The model was scaled corresponding to Froude length scale 1:61.5 which ensured an acceptable model size compared to the size of the flume and high density armour units being available. Furthermore, the Reynolds numbers for the armour units were acceptable for all sea states (fulfilling Eq. 1).

3.2 MATERIALS AND MODEL CONSTRUCTION

The tested cross-sections are proposals for the outer part of the western breakwater. The cross-sections consist of a core, upper core and high density rock armour layer.

3.2.1 Cross-Sections of the Rubble Mound Breakwater Proposed by Client

The proposed cross-sections supplied by the client are presented in Figs. 2 and 3. Cross-section C1 was the original proposal supplied by the client. Cross-section C2 was an additional proposal with a wider toe proposed by the client based on C1 results.

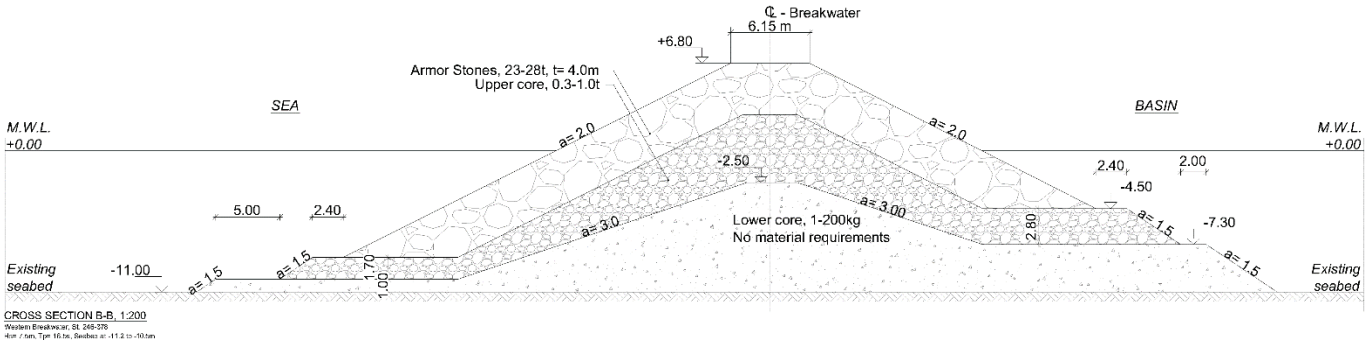

Figure 2: Cross-section proposed by the client, C1.

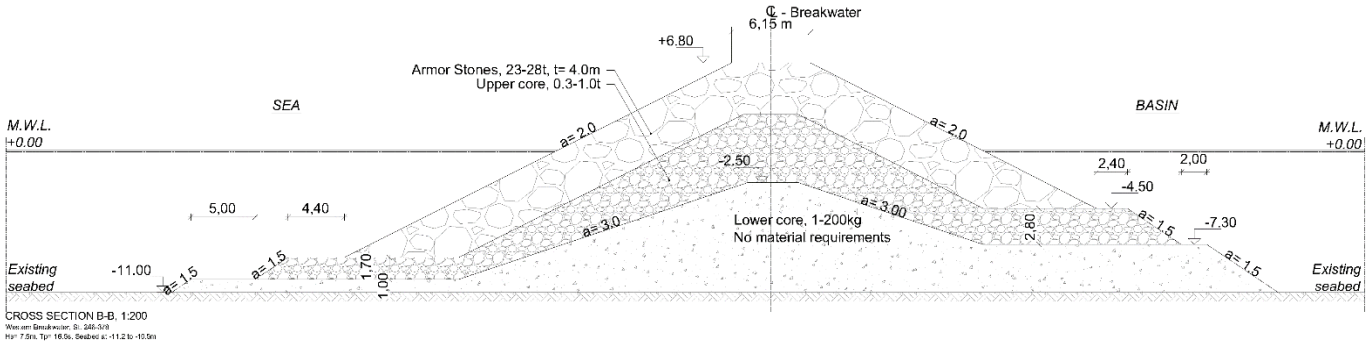

Figure 3: Cross-section proposed by the client, C2.

3.2.2 Definition of Stability Number

The tests were carried out in fresh water ($\rho \approx 1{,}000$ kg/m^3). In order to obtain the same armour hydraulic stability in sea water ($\rho = 1{,}025$ kg/m^3), it is necessary to compensate by keeping the term $\Delta D_{n,\,50}$ in the stability number identical in model and prototype.

$$N_s = \left(\frac{H_{1/3}}{\Delta D_{n,\,50}}\right) \tag{2}$$

where:

$$\Delta = \frac{\rho_a}{\rho_w} - 1 \tag{3}$$

$$D_{n,\,50} = \left(\frac{W_{50}}{\rho_a}\right)^{\frac{1}{3}} \tag{4}$$

N_s	stability number,
$H_{1/3}$	significant wave height at the toe of the breakwater,
Δ	relative density corrected for buoyance,
ρ_a	mass density of the armour units,
ρ_w	mass density of the water,
$D_{n,\,50}$	nominal armour unit size exceeded by 50% of the units,
W_{50}	is the mass of the units.

3.2.3 Armour, Upper Core and Core Material

Table 2 shows the material characteristics of the core, upper core and armour rocks. The sieve curves for the core, upper core and armour are given in Figs. 4 and 5. The rock armour size in the model was 3% larger than in prototype. This corresponds to a rock density of 3.04 t/m^3 in prototype which is still conservative for Norit (i.e. lower than what is used as basis for the design). Furthermore, the filter stone size when correcting for density was in the model 16% smaller than in prototype which is conservative for the stability of the toe. The size of the filter material was based on keeping the permeability similar in model and prototype.

Table 2: Model material.

Element	Target mass density, ρ_a [t/m^3]	Actual mass density, ρ_a [t/m^3]	Target W_{50} [t]	Actual W_{50} [t]	Target W_{15}-W_{85} [t]	Actual W_{15}-W_{85} [t]	Target D_{n50} [m]	Actual D_{n50} [m]	Actual D_{n85}/D_{n15}	Target ΔD_{n50}	Actual ΔD_{n50}
Armour	3.0	2.97	25.5	25.4	23.0-28.0	22.1-29.1	2.04	2.04	1.10	3.93	4.03
Upper core	3.0	2.49	0.65	0.76	0.30-1.00	0.44-1.20	0.60	0.67	1.40	1.16	1.00
Core	2.6	3.06	0.10	0.11	0.00-0.20	0.05-0.20	0.34	0.33	1.60	-	-

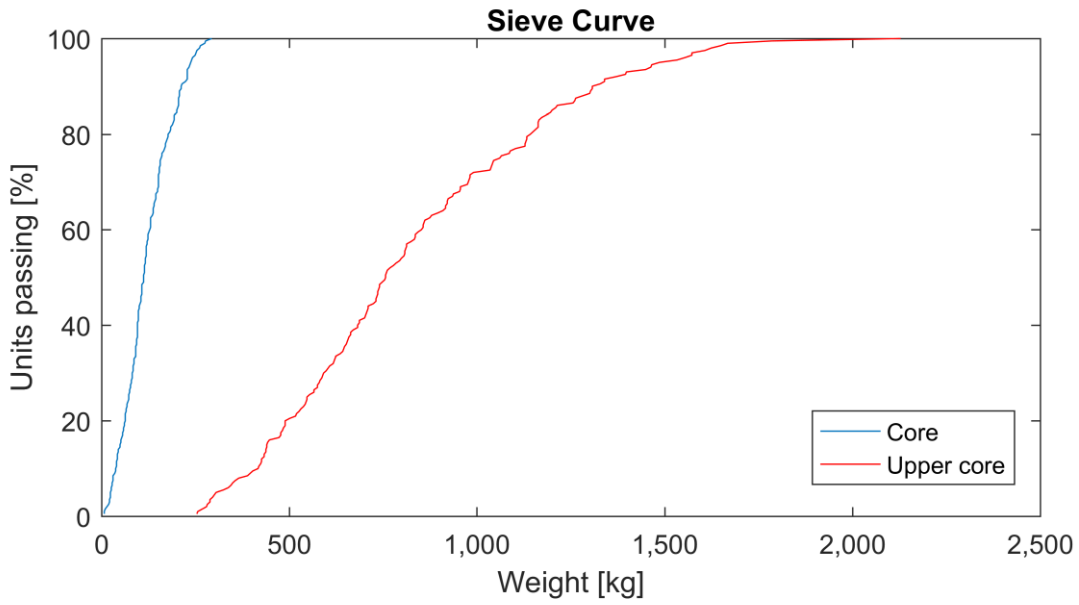

Figure 4: Sieve curve for core and upper core material.

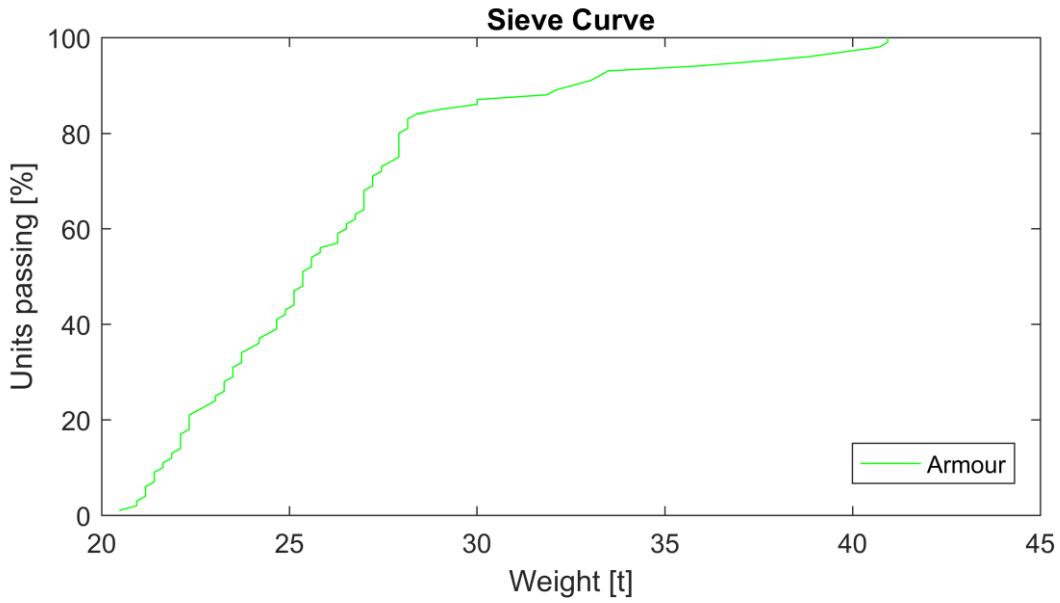

Figure 5: Sieve curve for the armour material.

3.2.4 Model Construction

The phases of construction of cross-section C1 are shown in Figs. 6 – 8. A final setup of C2 can be seen in Fig. 19. The foreshore was modelled together with a section of the breakwater. The first 12 m of the foreshore was made of plywood and the last 1.6 m was made of fine sand with $D_{n50} \approx 0.17$ mm in model scale (chosen to avoid cohesive response). The armour stones were placed in two layers and profile was measured with the laser profiler to ensure that the averaged profile was a close match to the design profile given by the client.

Figure 6: Breakwater with core and upper core for cross-section C1.

Figure 7: Breakwater with armour layer for cross-section C1.

Figure 8: Final setup without water for cross-section C1.

3.3 Principles of Measurements and Analysis

The waves were generated with a piston type wavemaker and the waves were measured with three arrays of wave gauges. The damage on the breakwater was measured with the laser profiler and supplemented by photo overlay from two cameras. The overtopping was measured by collecting the overtopping water in a tank.

3.3.1 Wave Generation

The waves were generated using the AwaSys 7 software (Aalborg University 2016a). The InvFFT – Random Phase generation technique was chosen. Second order wave paddle motion based on Schäffer and Stenberg (2003) was used. The use of second order wavemaker theory can also produce unreliable results if used in too shallow water, but by following the recommendations by Eldrup and Lykke Andersen (2016a) second order wave generation was found valid for all tests when taking into account the water depth at the paddle. Active absorption based on digital filtering of signals from two wave gauges positioned on the paddle face were used (Lykke Andersen et. al (2016)). The duration of each test was approximately 3 hours corresponding to app. 720 waves. The first order part of the spectrum was generated from a JONSWAP spectrum with a peak enhancement parameter, $\gamma = 3.3$.

3.3.2 Incident Waves in Front of the Breakwater and Wave Reflection

The data acquisition was done with a sample frequency of 100 Hz using a NI6225 acquisition box and the WaveLab 3 software package (Aalborg University 2016b). Analysis of the waves were performed with WaveLab 3. The wave gauges were calibrated using WaveLab 3 before each test run. The measured surface elevation time series from the gauge were analysed and split into incident and reflected waves using the nonlinear separation method by Eldrup and Lykke Andersen (2016b). A photo of the wave gauge array close to the toe is shown in Fig. 9. In Tests 12-14 a wave gauge was placed at the toe to measure the wave height distribution of the total surface elevation.

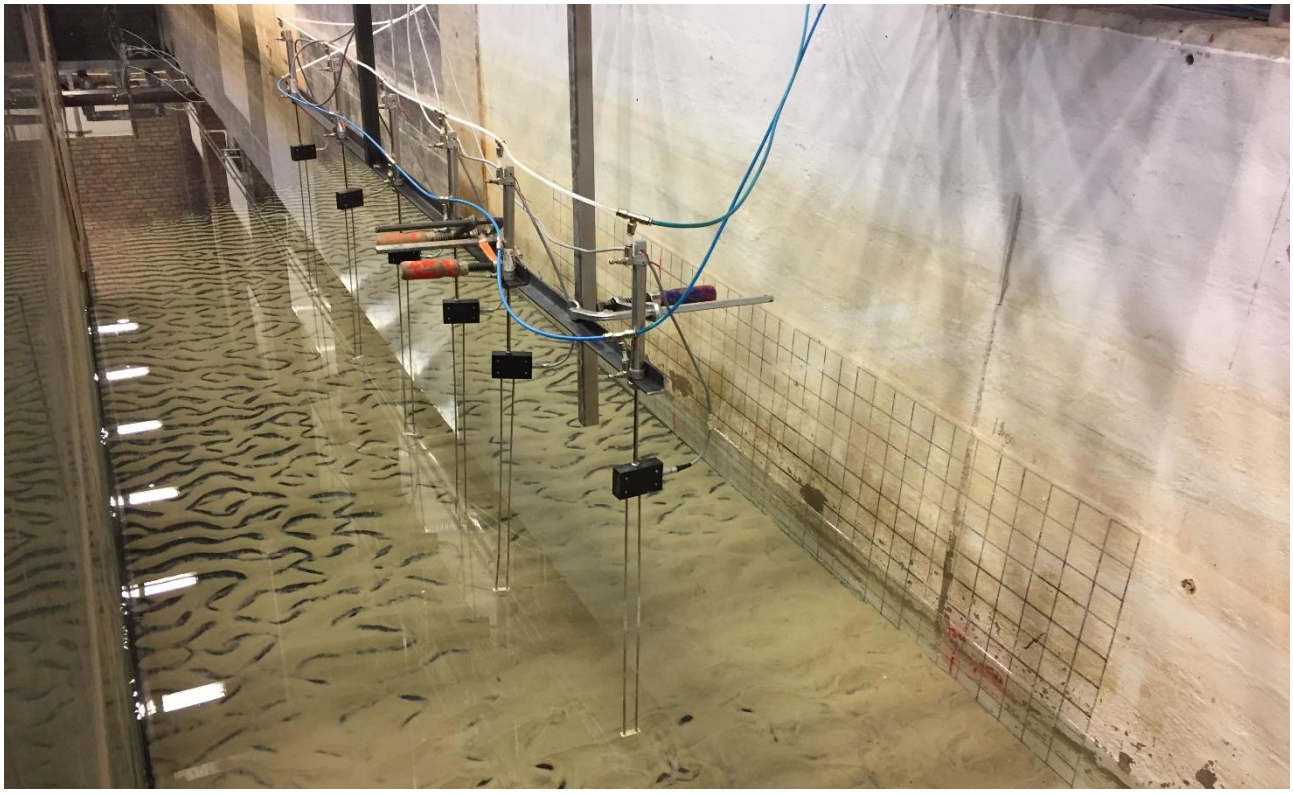

Figure 9: Wave gauges in front of the breakwater.

In Table 3 the target wave heights and the actual measured wave heights are presented for each test. Note that only low water level was tested for cross-section C2 as the purpose was to study stability of the wider toe. Before Test 12 the front armour was removed and the seabed, toe and front armour was rebuilt.

3.3.3 Measurement of Transmitted Waves

Transmitted waves are calculated based on the incident waves determined by the three gauges behind the breakwater using the Zelt and Skjelbreia (1992) method. As the transmitted surface elevations consist of setup and following draining (long waves) and normal waves a bandpass filter with limits 0.025 and 0.4 Hz has been applied for this analysis in order to calculate the normal waves.

Table 3: Test programme with target (input for wavemaker) and obtained wave heights in meters and periods in seconds.

Test no.	Cross-section	Target sea state	WL [m]	Target H_{m0} at buoy	Actual H_{m0} at buoy	Actual H_{m0}, h = 16.5	Actual $H_{1/3}$, h = 16.5	Actual H_{m0}/h, h = 16.5	Actual H_{max}/h, h = 16.5	Actual $H_{2\%}/H_{1/3}$, h = 16.5	Actual total $H_{2\%}/H_{1/3}$, toe	Actual $H_{1/3,t}$	Trans. coef. C_t = $H_{1/3,t}$ / $H_{1/3,i}$	Refl. coef. C_r = $H_{1/3,r}$ / $H_{1/3,i}$	Actual T_m, h = 16.5	Target T_P	Actual T_P, h = 16.5	Actual $T_{-1,0}$, h = 16.5	Actual $T_{0,1}$, h = 16.5	Actual $T_{0,2}$, h = 16.5
1	C1	S1	-0.5	5.2	5.29	5.33	5.51	0.33	0.70	1.42	-	0.22	0.04	0.34	12.2	15.0	14.6	14.2	11.3	10.2
2	C1	S2	1.3	5.2	5.30	5.35	5.38	0.30	0.64	1.46	-	0.48	0.09	0.37	12.1	15.0	14.6	14.2	11.5	10.4
3	C1	S3	1.7	5.2	5.31	5.36	5.30	0.29	0.53	1.44	-	0.60	0.11	0.37	11.8	15.0	14.6	14.1	11.6	10.5
4	C1	S4	-0.5	6.5	6.36	6.39	6.83	0.40	0.77	1.35	-	0.30	0.04	0.33	13.0	16.0	15.7	15.2	11.4	10.0
5	C1	S5	1.3	6.5	6.27	6.35	6.72	0.35	0.64	1.44	-	0.70	0.10	0.36	12.9	16.0	16.1	15.3	11.7	10.3
6	C1	S6	1.7	6.5	6.59	6.62	7.03	0.36	0.77	1.43	-	0.89	0.13	0.36	12.8	16.0	16.1	15.6	11.8	10.3
7	C1	S7	-0.5	8.2	7.96	7.98	8.67	0.50	0.79	1.26	-	0.53	0.06	0.33	13.4	16.5	16.9	16.7	11.2	9.5
8	C1	S8	1.3	8.2	7.92	8.03	8.79	0.44	0.76	1.31	-	1.06	0.12	0.33	13.2	16.5	16.1	16.2	11.4	9.8
9	C1	S9	1.7	8.2	8.25	8.32	8.92	0.45	0.78	1.29	-	1.33	0.15	0.34	13.4	16.5	16.5	16.3	11.7	10.1
10	C1	S10	-1	8.2	7.85	7.86	8.71	0.51	0.82	1.28	-	0.55	0.06	0.34	14.2	18.0	18.4	17.3	11.7	9.7
11	C1	S11	2.5	8.2	8.21	8.25	8.91	0.43	0.72	1.34	-	1.92	0.22	0.35	14.6	18.0	17.4	17.5	12.5	10.7
12	C2	S1	-0.5	5.2	5.38	5.47	5.58	0.34	0.73	1.44	1.30	0.20	0.04	0.35	12.2	15.0	15.3	14.0	11.2	10.1
13	C2	S4	-0.5	6.5	6.63	6.71	7.23	0.41	0.75	1.38	1.22	0.34	0.05	0.34	12.5	16.0	16.5	15.0	11.2	9.8
14	C2	S7	-0.5	8.2	7.98	7.97	8.74	0.50	0.75	1.21	1.22	0.50	0.06	0.34	13.2	16.5	16.5	16.0	11.1	9.4

3.3.4 Damage Detection and Hydraulic Stability

Damage of the front slope and crest was measured by a profiler (see Fig. 10) after each test. The rear side of the breakwater was only measured with the profiler for the 100 years return periods and overload cases. The reason for this was that the overtopping ramp was removed for these tests as it was more important to register the rear slope damage over the entire width than the amount of overtopping for these cases, while for the lower return periods it was more important to measure the overtopping also. Additionally, before pictures and after pictures of the breakwater was taken with two GoPro 5 cameras for photo overlay to visually see the damage, see Fig 11. The measured damage for each cross-section is the accumulative damage as the breakwater was not rebuild during the test programme.

Figure 10: Profiler used to measure eroded area on the breakwater, example with cross-section C1.

With the profiler, the eroded area was measured, and the damage level was calculated by Eq. 5.

$$S_{\mathrm{d}} = \frac{A}{D_{\mathrm{n,50}}^2} \tag{5}$$

Where:

S_{d} is the dimensionless damage level,

A is the eroded cross-sectional area,

Figure 11: Camera in front of the breakwater, example with cross-section C1.

4 STABILITY RESULTS

For the hydraulic stability, the breakwater is separated into three areas, front slope, crest and rear slope.

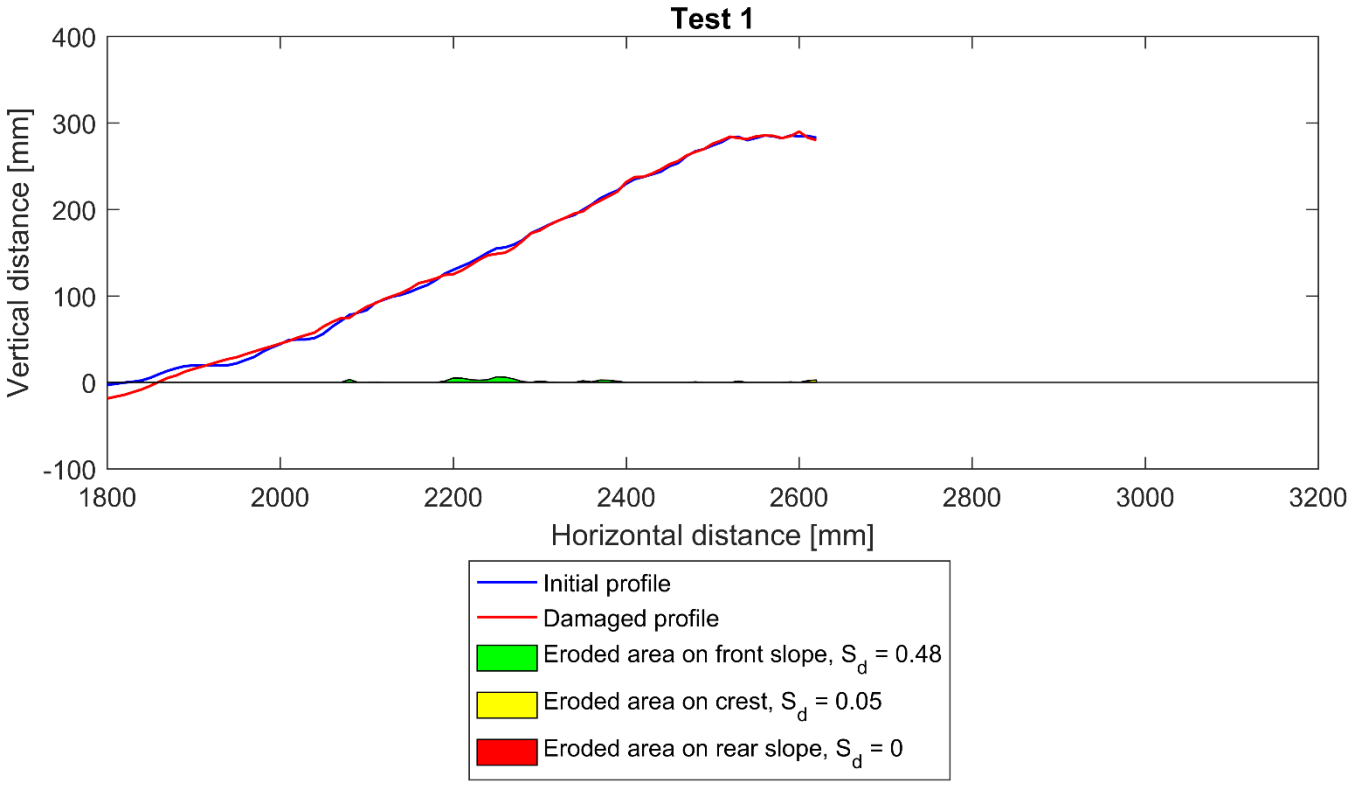

Figure 12: Example of measured average cross-section and calculated eroded area for Test 1 (model scale).

The damage given from the laser profiler is only considering the armour layer (front slope, crest and rear slope). It was not possible to measure the damage on the toe with the profiler as armour stones deposited here would lead to unreliable results. The measured damage can be seen in Table 4. After Test 11 the front and the crest of the breakwater was rebuilt, but the rear had still changed slightly shape under the reconstruction. Therefore, the initial profile before Test 12 is used to calculate all S_d values for Tests 12-14 also for the rear side.

Table 4: Stability results in terms of accumulated S_d after each test for front, crest and rear armour stones.

Test No.	$S_{d,\ front}$	$S_{d,\ crest}$	$S_{d,\ rear}$
1	0.48	0.05	-
2	0.52	0.07	-
3	0.95	0.09	-
4	0.69	0.06	-
5	0.81	0.06	-
6	0.92	0.07	-
7	1.51	0.15	0.82
8	1.57	0.14	1.00
9	1.85	0.23	1.10
10	2.02	0.24	1.21
11	2.21	0.31	1.44
12	0.47	0.09	0.10
13	0.75	0.05	0.19
14	1.07	0.09	0.36

For the toe stability photo overlay is used which showed that after the first test with cross-section C1 the toe was strongly flattened as shown in Fig. 12. Because of the damaged toe the armour layer had less support and might have observed additional damage due to this effect as a few armour stones slided down in front of the breakwater, cf. Fig 13.

Figure 13: The front of the breakwater (C1) is shown on both pictures. Left shows before tests and right shows after Test 1.

In Fig. 14 is the measured profile after Test 11 shown. The figure shows no critical damage to the armour layer with S_d around 2 for both front and rear armour. Note though that a part of the rear slope has been protected by the overtopping ramp in the first six tests.

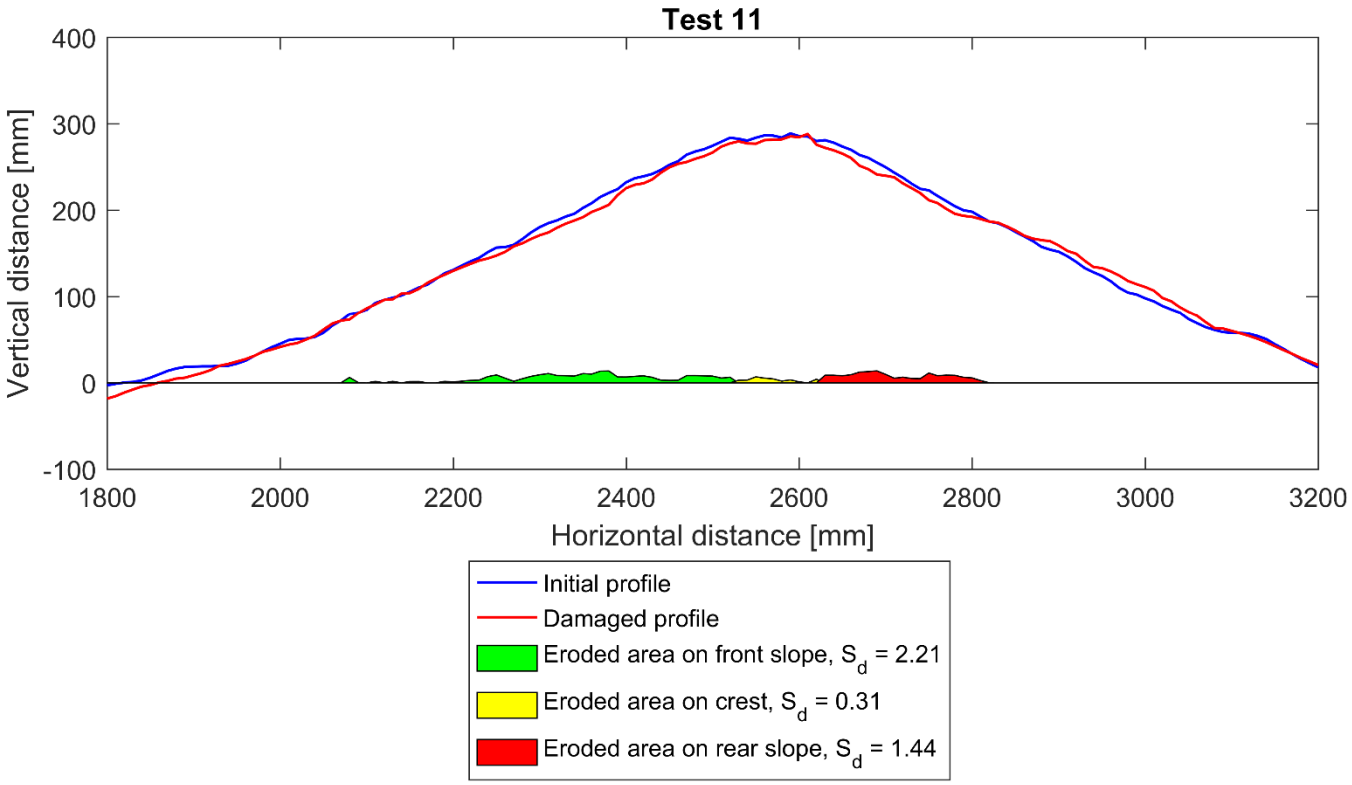

Figure 14: Measured average cross-section and calculated eroded area for Test 11 (model scale).

The front of the breakwater before testing and after the last test can be seen in Fig. 15. The figure shows that several stones from the front slope has slided down in front of the highly damaged toe, but except for the toe no critical damage can be observed on the front side of the breakwater.

Figure 15: The front of the breakwater (C1) is shown on both pictures. Left shows before tests and right shows after Test 11.

The damage to the rear side can be observed by comparing photos in Figs. 16 – 18. Damage could be observed after the 1 year events, but some damage is expected as the stones will settle when first exposed to waves/overtopping flow, cf. Fig 16. The damage increased after the 10 year events and could have been more severe if not the overtopping ramp protected the rear side as seen in Fig. 17. The damage after Test 11 is shown in Fig. 18. Some localized holes start to appear due to damage from high overtopping. However, the observed damage seems acceptable but some repair works must be expected after significant storms.

Figure 16: The rear of the breakwater (C1) is shown on both pictures. Left shows before test 1 and right shows after test 3.

Figure 17: The rear of the breakwater (C1) is shown on both pictures. Left shows before Test 1 and right shows after Test 6.

Figure 18: The rear of the breakwater (C1) is shown on both pictures. Left shows before Test 1 and right shows after Test 11.

4.1.1 Additional Cross-Section C2

After Test 11, the stability of the toe was not found acceptable. Therefore, a new cross-section with a wider toe was tested for sea state T1, T4 and T7. The damage after the three tests can be seen on Fig. 19. The toe provided a better protection, but still some armour stones slided down in front of the toe which also flattend very significantly.

Figure 19: The front of the breakwater (C2) is shown on both pictures. Left shows before Test 12 and right shows after Test 14.

5 OVERTOPPING RESULTS

During the tests the overtopping was measured. The overtopping was led to an overtopping tank (capacity $\simeq$ 21 l in model scale) via a ramp (width 30 cm in model scale) extending from the rear side of the crest. A wave gauge inside the tank was used to measure the water level inside the tank. When the tank contained more than 15 l (model scale) a pump was configured to automatically start and empty the tank. Knowing the water level in the tank and the pump capacity and state (on/off), an overtopping discharge time series was calculated (see in Figure 20).

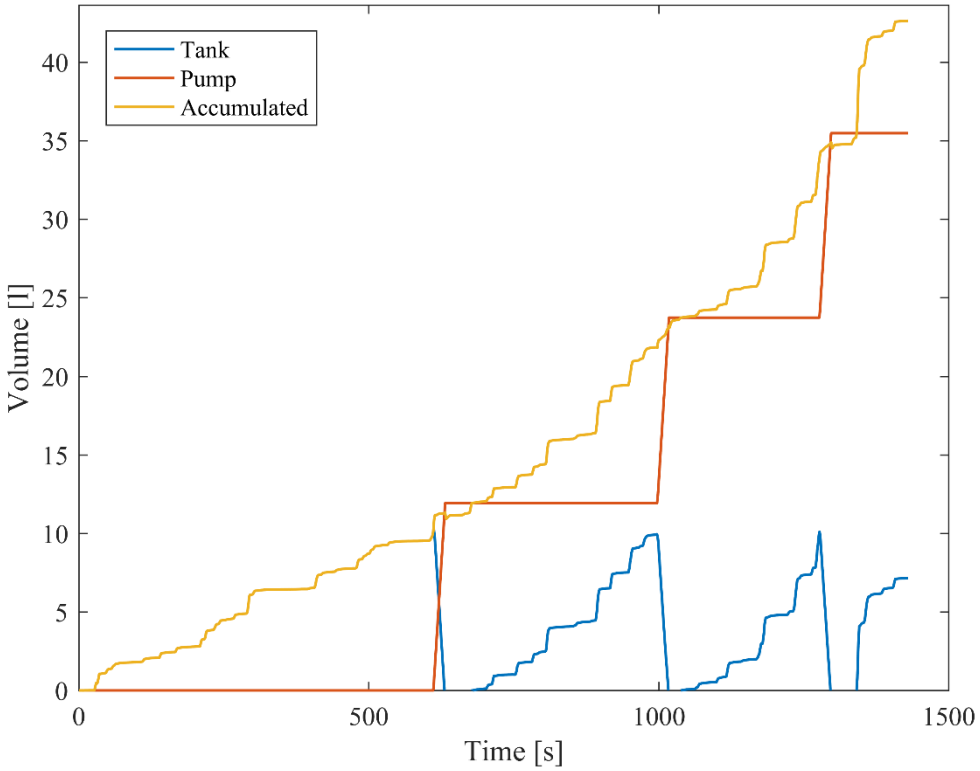

Figure 20: Example of measured overtopping (model scale).

There was measured up to 63 l/s/m overtopping for the 1 year events and 239 l/s/m overtopping for the 10 year events. As mentioned in earlier chapters the overtopping were not measured for the 100 year events and overload cases as it was found more important to measure damage on the rear side of the breakwater.

Table 7: Overtopping results.

Test No	$q_{,\text{measured}}$ [l/s/m]
1	15.0
2	49.0
3	62.7
4	33.1
5	147.3
6	238.8

The measured overtopping is compared to the predicted overtopping by CLASH Neural Network (Van Gent et al. (2007)) in Fig. 21. The methods show good agreement between the predicted and measured overtopping.

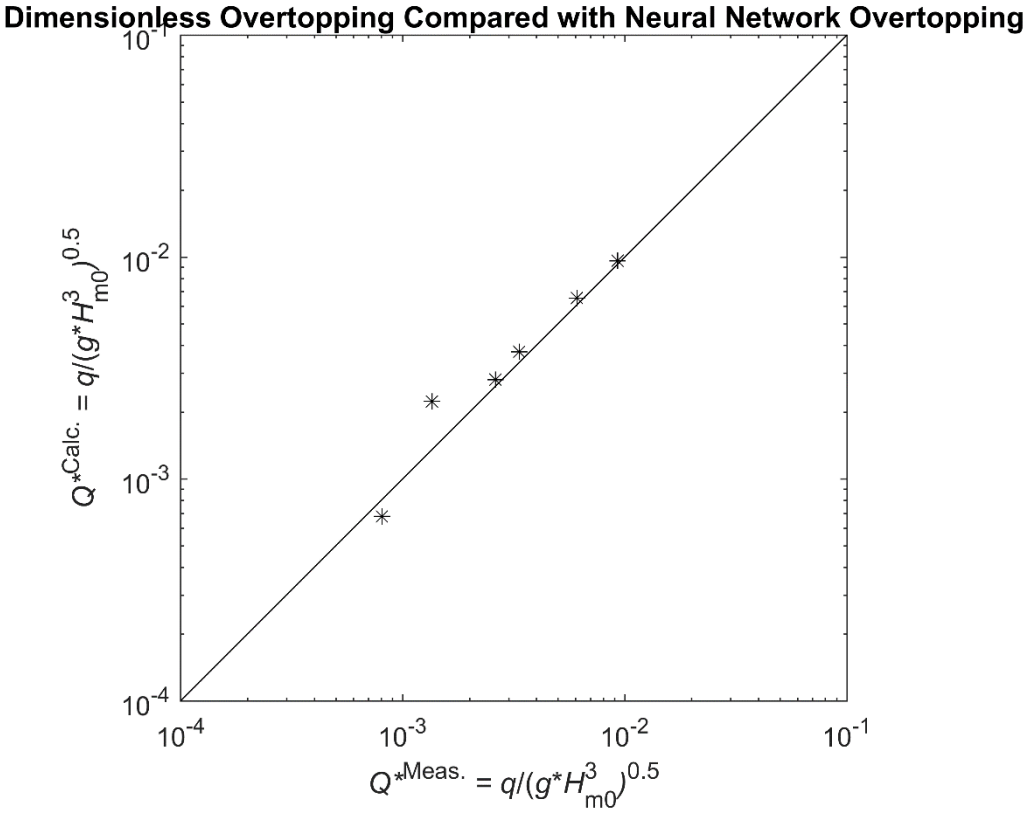

Figure 21: Measured overtopping compared to Neural Network Overtopping.

6 CONCLUSIONS

The proposed new western breakwater for port of Hanstholm expansion has been tested in the present work. The stability, overtopping and transmission of the cross-section was tested with 11 sea states provided by the client. After the tests both the front and rear armour layer had obtained damage corresponding to $S_d \approx 2$. Rear side showed some localized larger holes but filter was never exposed. The stability of the toe in C1 was not found acceptable with initial proposed cross-section as it was completely flattened after the 1 year storm. Therefore, a cross-section with a wider toe, C2, was tested. This cross-section showed also significant displacement of toe material. However, the armour layer support was much better than the narrow toe and the design is acceptable in the 2D tests. The overtopping was found to be in agreement with predictions by CLAHS Neural Network. The transmission coefficient for the 1 year and 10-year return periods was respectively up to 11% and 13%.

7 REFERENCES

Aalborg University (2016a) AwaSys homepage. http://hydrosoft.civil.aau.dk/AwaSys

Aalborg University (2016b) WaveLab 3 homepage. http://hydrosoft.civil.aau.dk/wavelab

Eldrup, M. R. and Lykke Andersen, T. (2016a). *"Applicability of Second Order Wavemaker Theory for Highly Nonlinear Waves"*. Submitted to Coastal Engineering for review.

Eldrup, M. R. and Lykke Andersen, T. (2016b). *"Estimation of Incident and Reflected Wave Trains in Highly Nonlinear Two-Dimensional Irregular Waves"*. Submitted to Coastal Engineering for review.

Klopman, G. and Van der Meer, J.W. (1999). "*Random wave measurements in front of reflective structures"*. Journal of WPC and OE, ASCE, Volume 1, No. 1, pp. 39-45. New York.

Lykke Andersen, T., Clavero, M., Frigaard, P., Losada, M., Puyol, J.I. 2016. *"A new active absorption system and its performance to linear and non-linear waves"*. Coastal Engineering, Volume 114, August 2016, Pages 47-60

Schäffer, H. A., and Steenberg, C. M. 2003. *"Second-order wavemaker theory for multidirectional waves"*. Ocean Engineering 30, pp 1203-1231.

Van Gent, M.R.A., van den Boogaard, H.F.P., Pozueta, B, Medina, J.R. 2007. *"Neural network modelling of wave overtopping at coastal structures".*

Zelt, J. A., and Skjelbreia, J. E. 1992. *"Estimating incident and reflected wave fields using an arbitrary number of wave gauges"*. Coastal Engineering Proceedings, 1(23).